



# Quench dynamics in MgB<sub>2</sub> Rutherford cables

A Cubero<sup>1</sup>, R Navarro<sup>1</sup>, P Kováč<sup>2</sup> , L Kopera<sup>2</sup>, M Rindfleisch<sup>3</sup> and E Martínez<sup>1,4</sup> 

<sup>1</sup>Instituto de Ciencia de Materiales de Aragón, CSIC—Universidad de Zaragoza, C/María de Luna 3, E-5018 Zaragoza, Spain

<sup>2</sup>Institute of Electrical Engineering, Slovak Academy of Sciences, Dúbravská cesta 9, 841 04 Bratislava, Slovakia

<sup>3</sup>HyperTech Research, Inc., Columbus, OH 43210, United States of America

E-mail: [elenamar@unizar.es](mailto:elenamar@unizar.es)

Received 16 January 2018, revised 7 February 2018

Accepted for publication 20 February 2018

Published 9 March 2018



## Abstract

The generation and propagation of quench induced by a local heat disturbance or by overcurrents in MgB<sub>2</sub> Rutherford cables have been studied experimentally. The analysed cable is composed of 12 strands of monocoil MgB<sub>2</sub>/Nb/Cu10Ni wire and has a transposition length of about 27 mm. Measurements of intra- and inter-strand voltages have been performed to analyse the superconducting-to-normal transition behaviour of these cables during quench. In case of external hot-spots, two different time-dynamic regimes have been observed, a slow stage for the formation of the minimum propagation zone (MPZ), and a fast dynamics once the quench is triggered and propagates to the rest of the cable. Significant local variations of the quench propagation velocity across the strands around the MPZ have been observed, but with average quench propagation velocities closely correlated with the predictions given by one-dimensional-geometry models. For quench induced by overcurrents (i.e. with applied currents higher than the critical current) the nucleation of many normal zones distributed within the cable, which overlap during quench propagation, gives a distinctive and faster quench dynamics.

Keywords: MgB<sub>2</sub>, Rutherford cables, quench, thermal stability, superconductor

(Some figures may appear in colour only in the online journal)

## 1. Introduction

Rutherford-type cables based on low temperature superconductors (LTS) NbTi and Nb<sub>3</sub>Sn, have been widely used in the past several years to build magnets for high-energy physics [1, 2]. Compared to monolithic conductors, these cables have high strand packing and fully transposed current paths, which allows a substantial increase of current capability together with a reduction of AC losses. Thus, by using these cables, the magnet inductance, the operating voltage, and the magnetic energy stored in the system can be reduced, which is of great relevance for these large-scale applications.

Initially, one of the main drivers for superconducting Rutherford cables was the development of NbTi dipole and

quadrupole magnets for particle accelerators. Later on, the interest in Rutherford cables was extended to other superconducting materials and applications. In this way, cables that allows higher operating magnetic fields and/or temperatures, based on Nb<sub>3</sub>Sn [2, 3], Bi<sub>2</sub>Sr<sub>2</sub>CaCu<sub>2</sub>O<sub>8+x</sub> [4–6], and more recently MgB<sub>2</sub> [7, 8] and coated conductors [9], have already been developed. Certainly, the specific mechanical, chemical and physical characteristics of the superconducting wires or tapes used for cabling create particular challenges and impose different cabling strategies. On the other hand, prototypes of superconducting magnetic energy systems [10, 11] and very high-field magnets [12], have already been manufactured using Rutherford cables.

Braided or twisted cables are often required in many applications to achieve a reduction of the AC losses when using appropriate transposition length and inter-strand

<sup>4</sup> Author to whom any correspondence should be addressed.

**Table 1.** Characteristics of analysed  $\text{MgB}_2$  Rutherford cable (samples RC-1 and RC-2) and of one isolated strand extracted from the cable.  $I_c$  is the critical current at self-field and  $R$  the resistance per unit length.

Sample ID	Transversal dimensions	$I_c$ (A)			$R$ ( $\text{m}\Omega \text{ cm}^{-1}$ )		Description
		$T = 35 \text{ K}$	33 K	32 K	$T = 40 \text{ K}$	293 K	
RC-1	$0.7 \text{ mm} \times 2.7 \text{ mm}$	69	—	170	0.16	—	Cable with 12 strands and transposition length $L_p \sim 27 \text{ mm}$
RC-2	$0.7 \text{ mm} \times 2.7 \text{ mm}$	110	220	—			
Strand	$\sim 0.12 \text{ mm}^2$	8.5	19	21	1.9	16	Monocore $\text{MgB}_2/\text{Nb}/\text{Cu10Ni}$

electrical resistance [13–16]. In the presence of alternating fields or during magnet field ramping, coupling currents are induced that loop around a half-pitch of the cable and through the crossover and adjacent strands. Therefore, increasing the contact electrical resistance between strands is beneficial for decreasing AC losses, although on the other hand, as the current transfer among strands reduces, so does the thermal stability of the cable. Therefore, the optimization process of the cables should take into account both mentioned opposing effects, although the optimum balance may differ for each particular application.

The thermal stability of different designs of LTS Rutherford cables has been analysed by several groups [17–22], where the effect on quench characteristics of strand coating, individually insulated strands, contact resistance between strands, as well as the presence of a resistive core inside the cable (between the upper and lower layers of the cable) has been studied.

Since Rutherford cables based on  $\text{MgB}_2$  have just been recently proposed [7, 8] and are not yet fully developed, it is important to understand their behaviour to further optimize their superconducting properties while providing the required thermal stability for the different applications. The present work aims to analyse the quench dynamics of  $\text{MgB}_2$  Rutherford cables, especially focussing on the quench induced by a local heat disturbance. The analysed cable has 12 strands and a transposition length of about 27 mm and was manufactured using monocore  $\text{MgB}_2/\text{Nb}/\text{Cu10Ni}$  round composite wires. During a quench, measurements of the voltages along given strands and between different strands have been performed and analysed to understand the superconducting-to-normal transition characteristics during a quench induced by hot-spots or overcurrents. A further analysis of the experimentally estimated global quench propagation velocities in terms of simple one-dimensional conductor models has been done.

## 2. Experimental

The characteristics of the Rutherford cable analysed in this study are collected in table 1. The cables have 12 strands and rectangular cross section of dimensions 2.7 mm wide by  $\sim 0.7 \text{ mm}$  thick. The transposition length, also referred to as the transposition pitch, is  $\sim 27 \text{ mm}$ . The cable was made from

monocore wires with undoped Mg and B precursors and Cu10Ni alloy as outer sheath. The used wires were cold drawn down to 0.39 mm and have Nb barrier between the superconducting core and the sheath. After the final cable manufacturing, *in situ* reaction of the  $\text{Mg} + \text{B}$  precursor powders to form the superconducting  $\text{MgB}_2$  phase was done at  $650^\circ\text{C}$  for 30 min in Ar atmosphere. The wires were manufactured by HyperTech Research and the cabling was performed in the Institute of Electrical Engineering of Bratislava. The cabling procedure and the superconducting properties of Rutherford cable and wire are described in detail in [8].

Both analysed samples, RC-1 and RC-2, of length 11 cm, come from the same cable and therefore have similar manufacturing procedure, except that RC-1 was heat treated at  $650^\circ\text{C}$  with a bend diameter of 80 mm and subsequently straightened, while RC-2 was directly heated in straight form. Before the final reaction heat treatment, a strand was extracted from another piece of the same cable and subsequently heated at the same conditions ( $650^\circ\text{C}$  for 30 min). The measured critical currents of a 5 cm-long segment of this single strand,  $I_{c,\text{strand}}$ , are also collected in table 1. Thus, the critical currents of cable RC-2 are about 12 times  $I_{c,\text{strand}}$ , as expected for a cable with rather homogenous strands. On the contrary, the smaller  $I_c$  values of cable RC-1 suggest a certain deterioration of this cable, probably due to the straightening process after heat treatment.

All measurements were performed with the samples in vacuum and cooled by conduction from both ends (current-feeding contacts), which were thermally anchored to the second stage of the used cryocooler. A thermometer was glued to the cable to control the initial temperature of the sample,  $T_0$ , before quench measurements. This operating temperature was controlled with a Lakeshore temperature controller.

For quench measurements under local heat disturbances, the energy was deposited to the cable, carrying a current,  $I < I_c(T_0)$ , by passing a rectangular current pulse of variable duration in a heater. This input energy is increased in small steps by increasing either the current or the duration of the pulse,  $t_p$ , estimating this way the minimum energy able to trigger the quench of the cable (minimum quench energy). Usually, to simulate local heat disturbances in cables, either carbon-paste heaters attached to a single strand [17, 18] or heaters that spanned over the width of the cable [20] have

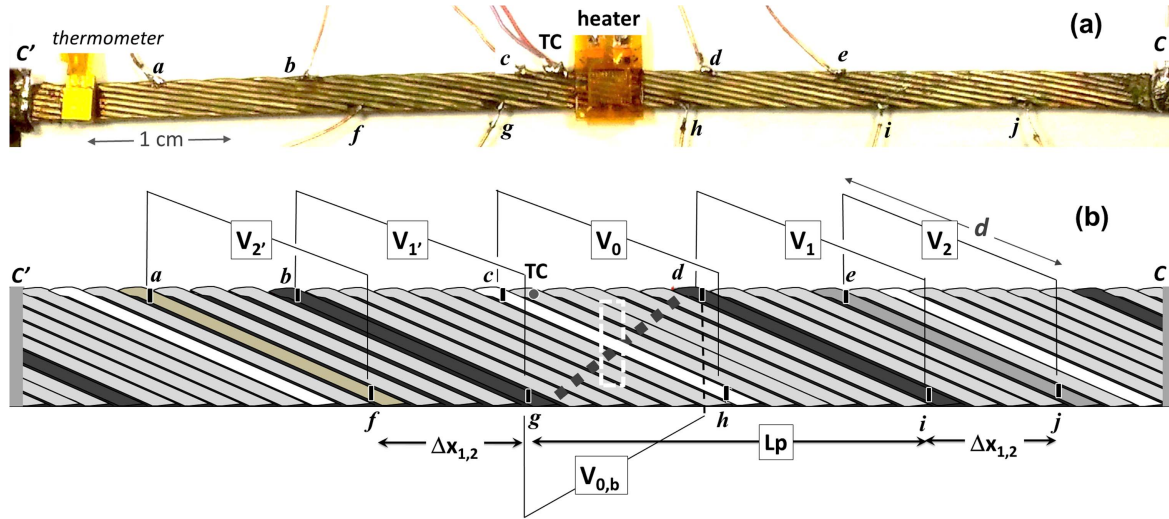


**Figure 1.** (a) Photograph of Rutherford cable RC-2 showing the heater, ten voltage taps (a–j) and a thermocouple (TC). (b) Scheme of the same cable (drawn wider than real for clarity purposes) showing some highlighted strands, heater position, voltage taps and some measured voltages:  $V_0$  (between taps c and h),  $V_{0,b}$  (g–d),  $V_1$  (d–i),  $V_2$  (e–j), etc. The total length of the measured cable is 11 cm and the distance between global voltage taps C' and C is 8 cm,  $\Delta x_{1,2} \sim 1$  cm and  $d \sim 1.2-1.3$  cm.

been previously used. Here, a strain gage of resistance  $120 \Omega$  and dimensions  $3 \text{ mm} \times 2 \text{ mm}$  on a  $20 \mu\text{m}$ -thick Kapton foil is used as heater. It was glued to the surface of the cable, at mid distance between current contacts, and overlaps five strands.

Several voltage taps were used to analyse the development and propagation of the quench. Unlike most monolithic conductors, where the full cross section at a given position  $x_0$  ( $0 < x_0 < L$ , where  $L$  is the length) can be considered equipotential in a good approximation [23], for  $\text{MgB}_2$  Rutherford cables this assumption is not always valid and the measured voltages may depend on the relative position of voltage taps between the strands, as it will be discussed later. Thus, the quench analysis may become very complicated by using in these multistrand cables, the same voltage taps' disposition as in monolithic conductors [23, 24]. On the other hand, global voltage taps, which are in electrical contact with all the strands at a given cross section, were disregarded, except for measuring the total voltage of the cable, because they would provide additional electrical and thermal paths and therefore, they would change the real conditions of the cable.

Although different arrangements of voltage taps were tried in preliminary tests, due to the above-mentioned reasons, the tap configuration shown in figure 1 has been chosen, following a procedure similar to that proposed by Willering *et al* [21, 22]. In this configuration all the voltages given in the figure are measured between two taps soldered in a given strand (the distance between each pair of taps following the strand is  $d \sim 1.2-1.3$  cm). This way,  $V_0$  and  $V_{0,b}$  correspond to the voltages measured in the heater area in segments of two strands that are symmetrically crossed. The former is at the top side of the cable, in direct contact with the heater, and the latter at the bottom. Since taps b, g, d and i are soldered in the same strand, voltages  $V_1$  and  $V_{1'}$  are measured in symmetric segments of the same strand sensed by  $V_{0,b}$ , at the right- and the left-hand side of the heater, respectively. At a distance of

$L_p/2 + \Delta x_{1,2}$  ( $\Delta x_{1,2} \sim 1$  cm), 10 strands away from the central strand section sensed by  $V_0$ , voltages  $V_2$  and  $V_{2'}$  are measured in two different strands, which are farther away and also in symmetric positions around the heater. Note that these two strands are not in direct contact with the heater, neither sensed by any other tap. Finally, the total voltage of the cable,  $V_{\text{cable}}$ , is measured between two global taps, C' and C, which are close to the current contacts. These taps, separated by a distance of 8 cm, connect electrically all the strands at cross sections C and C' by means of Sn–Pb–Ag solder. In the experiments, all voltages are always measured using the same polarity, left–right, in such a way that in the normal state all measured voltages are positive.

A thermocouple (TC) was also attached to measure the temperature near the hot-spot. The voltages between different taps and the temperature measured by the TC were recorded using a data acquisition device. The experiment is controlled through LabVIEW graphical interface. In order to protect the cables during a quench the power supply is switched-off via GPIB when the total voltage measured in the cable reaches a value of 80–100 mV.

### 3. Results and discussion

Two similar samples RC-1 and RC-2, with different critical currents (see table 1), were measured at different temperatures and currents. Nevertheless, since RC-1 suffered some deterioration, in this paper the detailed analysis of the voltage development during quench has been focussed on cable RC-2, as it is more relevant. However some results of cable RC-1 have also been reported and analysed.

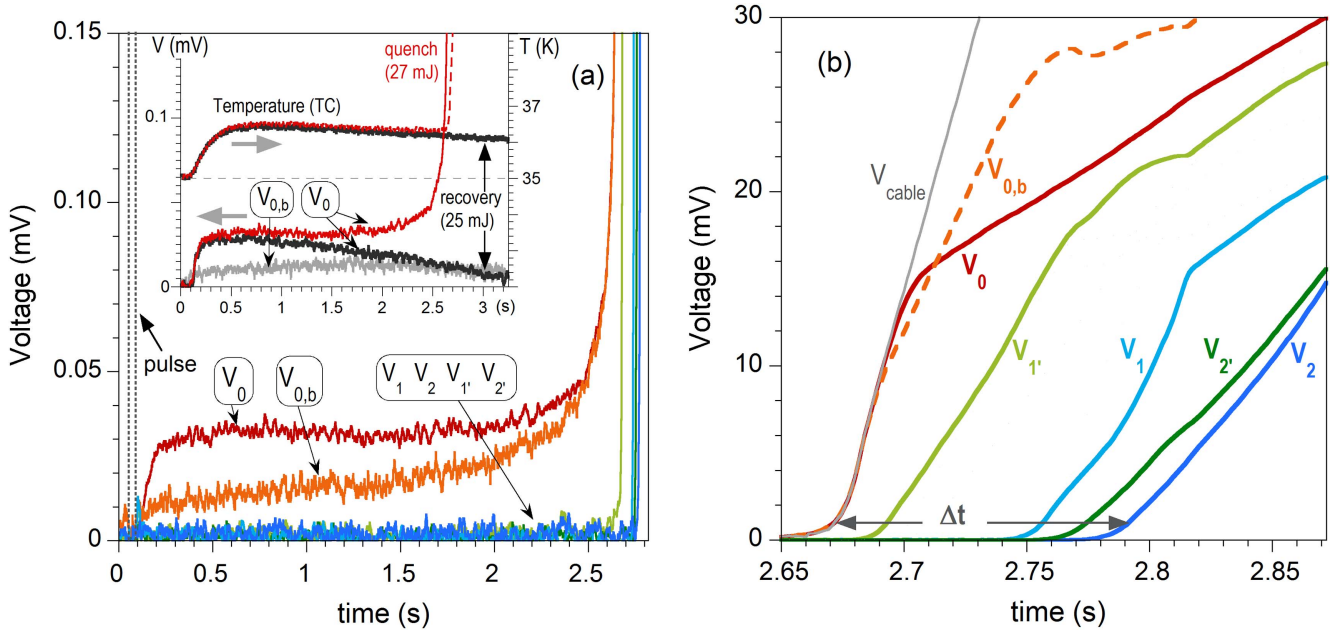


**Figure 2.** Time evolution of the different voltages, named as in figure 1(b), measured in cable RC-2 during quench at  $T_0 = 35$  K and  $I = 82$  A. (a) Detail of the initial stages of quench development. Inset: Comparison of the time evolution of voltages and temperature near the heater for quench and recovery cases (temperature was measured by thermocouple TC).  $V_{0,b}(t)$  in case of recovery, is also shown for comparison. (b) Voltages measured during quench propagation.  $\Delta t$  is the time delay between  $V_0(t)$  and  $V_2(t)$  at voltage values of 1 mV. Note that the time- and voltage-scales are different in (a) and (b).

### 3.1. Development of quench induced by local heat disturbances

Figure 2(a) shows the time evolution of the voltages measured in cable RC-2 after a heat pulse of energy 27 mJ and duration 40 ms, which induces a quench. Recovery is observed after applying slightly lower energy, 25 mJ, in a pulse of the same duration. The inset of the figure shows the comparison of voltage and temperature time evolution near the hot-spot, in the events of quench and recovery. In case of quench, the heat pulse produces a metastable state, with voltage value  $V_0(t)$  almost constant  $\sim 30 \mu\text{V}$  for about 2 s, which eventually results in a fast increase of the voltage. During this metastable state, the temperature measured by the TC is about 36.5 K, just 1.5 K above the initial temperature  $T_0 = 35$  K and below the critical temperature,  $T_c \sim 38$  K. Within the strand, current sharing between the superconducting core and the metal sheath (current-sharing regime) would be present at this stage.

Among all the measured voltages, only those at the heater area ( $V_0$  and  $V_{0,b}$ ) shows signal above noise level before the quench triggers. Nevertheless, while  $V_0(t)$  increases fast up to  $30 \mu\text{V}$  and remains almost constant,  $V_{0,b}(t)$  increases more slowly but continuously. Eventually, at  $t \sim 2.5$  s, both voltages equal and increase sharply at the same rate. This can be observed in figure 2(b), where the same voltages are plotted in an expanded time scale for better observation of the quench propagation dynamics. The time interval from the initial hot-spot to quench triggering is considerably longer than for monolithic conductors [23], which may be favoured by current redistribution among strands.

Attention should be paid to the coincidence of both voltages  $V_0$  and  $V_{0,b}$  with the total voltage  $V_{\text{cable}}(t)$  from the time of quench triggering (at  $t \sim 2.5$  s) until the onset of  $V_1(t)$  at  $t \sim 2.69$  s, which would be expected for parallel resistances with negligible current transfer between them. This behaviour differs in some aspects from the results obtained in NbTi Rutherford cables immersed in liquid helium at 4.3 K [22], although it is important to note that the differences between both experiments are not limited to the type of analysed samples and cooling conditions, but also to the way the heat is deposited. Willering *et al* [22] used a graphite paste heater positioned in a small section of a strand to induce the quench. They observed that the current of the normal conducting strand section created by the hot-spot is transferred to its neighbouring strands. Besides, voltages of several mV were measured in strands segments around the heater before measuring voltage by the global taps of the cable.

At later stages, there are some observations that suggest complex current transfer between strands. For example, voltage  $V_{0,b}(t)$  presents some fluctuations (it decreases at  $t \sim 2.76$  s before increasing again some ms later), which are not due to current variations in the cable. Besides, there are some differences in shape among the different  $V_i(t)$  curves during quench propagation, unlike the behaviour observed in single conductors, where all  $V_i(t)$  curves measured along the conductor during a quench are very similar, just displaced in time [23].

The above experimental results point-out two different time scales in quench dynamics. At the beginning, the formation of a minimum propagating zone (MPZ) is slow and dominated by the conductive heat flow from the strands in the upper part of the cable close to the heater, to those at the



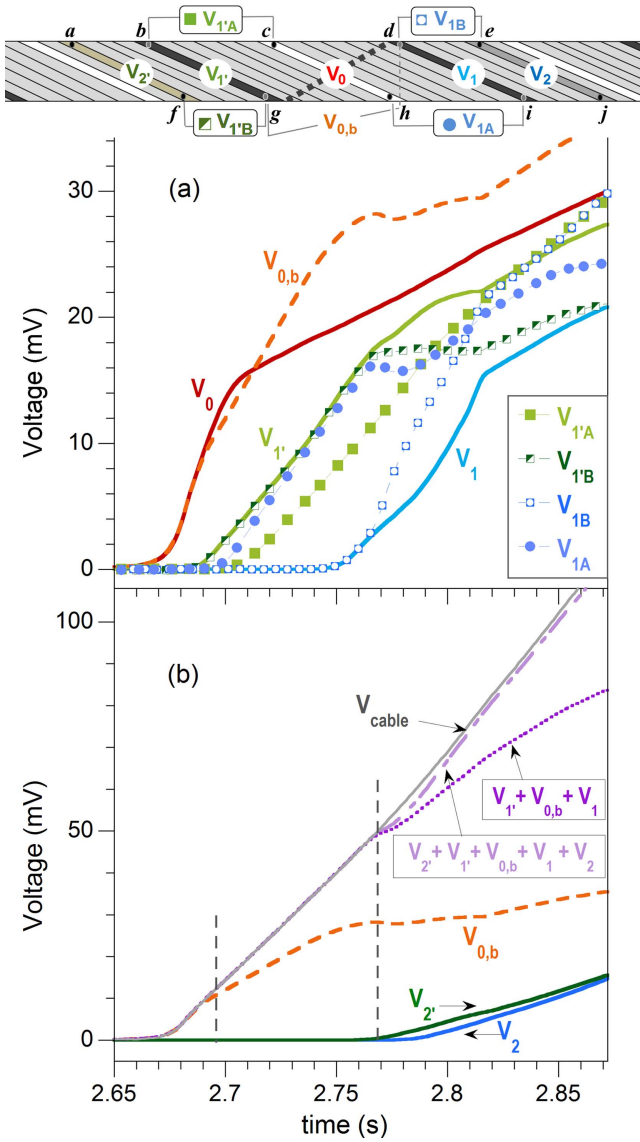


**Figure 3.** Time evolution of different voltages measured in cable RC-2 during the same quench as in figure 2. (a) Voltages measured across strands (symbols defined in the inset), and along given strands (lines without symbols). (b) Comparison between the total voltage ( $V_{cable}$ ) and the sum of different voltages measured in several strand segments.

bottom in contact with them. The formation of a MPZ, which includes several strands, triggers the quench that propagates to the rest of the cable on a shorter time scale. It is also remarkable that although the quench propagation is not symmetric around the heater, as there is a delay of  $\sim 63$  ms between the onset of voltages  $V_1(t)$  and  $V_{1'}(t)$ , this delay decreases considerably, down to 15 ms, between the filament segments more distant from the heater, which are sensed by voltages  $V_2(t)$  and  $V_{2'}(t)$ . This suggests that the presence of inhomogeneities in the local critical current of the strands, and/or in the thermal contact resistance among them, is evidenced mainly in the area close to the quench origin.

Further analysis of the first stages of quench evolution can be done by studying the voltages measured between taps of different strands as seen in figure 3(a). The onset of

voltages  $V_{1'A}(t)$  and  $V_{1A}(t)$ , which correspond to taps pairs (b, c) and (h, i), respectively, and have point of symmetry in the centre of the heater, occurs at the same time ( $t \sim 2.7$  s) and coincides with a change of the slope  $V_0(t)$  at  $\sim 15$  mV. This value corresponds to the voltage of an insulated strand of length equal to segment between taps c and h ( $d = 1.2$  cm) when carrying a current  $I/12$  at 40 K (normal state) and thus indicates that the quench arrives to taps c and h when the strand segment (c, h) is fully in the normal state.

On the other hand, voltages  $V_{1'B}(t)$  and  $V_{1B}(t)$ , which correspond to tap pairs (f, g) and (d, e) and also have point of symmetry in the centre of the heater, exactly coincide with  $V_1(t)$  and  $V_{1'}(t)$ , respectively, during the first stages. Therefore the quench in the strand segment sensed by  $V_1$  (between taps d and i) propagates from the upper to the lower edge but not from the cable centre towards the edges. Similarly, in the strand segment sensed by  $V_{1'}$  (taps b, g), quench propagates from the lower to the upper edge. Therefore, the quench propagation along each strand, following the 'twisted' geometry of the cable, would be predominant near the hot-spot.

For a better understanding of the quench behaviour, it is also interesting to compare the total voltage of the cable,  $V_{cable}(t)$ , with the sum of the voltages measured in several strand segments, as it is shown in figure 3(b). It must be remarked that since not all these intra-strand voltages have common references, their sum could differ from  $V_{cable}(t)$ . As it is shown in the figure, the whole  $V_{cable}(t)$  curve is almost coincident with the sum of voltages  $V_{2'}$ ,  $V_{1'}$ ,  $V_{0,b}$ ,  $V_1$  and  $V_2$ ; and three time intervals are clearly distinguished. First, for  $t < 2.7$  s, the total voltage overlaps with  $V_{0,b}$  (and  $V_0$ ), so that the normal zone in this time interval would be restricted to the cable region limited by taps c, d, g and h, in the centre of the cable. Furthermore,  $V_{cable}$  coincides with the sum of voltages  $V_{1'}$ ,  $V_{0,b}$  and  $V_1$  until  $t \sim 2.77$  s, moment when voltages  $V_2$  and  $V_{2'}$  start given signal. These results suggest that a normal zone is first created in the centre of the cable around the heater, and subsequently, the normal-superconducting front propagates towards the ends of the cable. In general terms, this is similar to the behaviour of monolithic conductors, although the cabling structure introduces complexity in quench propagation.

### 3.2. Quench propagation velocities

The quench propagation velocities can be estimated experimentally from the time delay between measured voltages in different strand segments (see figure 1) and the distance between corresponding voltage taps. Global quench propagation velocities were obtained as  $v_p = \Delta x / \Delta t$ , where  $\Delta t$  is the time delay between voltages  $V_0(t)$  and  $V_2(t)$  at a given voltage value,  $V_{\Delta}$ , and  $\Delta x$  is the distance between corresponding taps,  $\Delta x = \Delta x_{1,2} + L_p/2$  (figure 1(b)). As it is seen in figure 2(b),  $V_0(t)$  and  $V_2(t)$  curves are not parallel during the superconducting-to-normal transition of the sensed strand segments. The time delay  $\Delta t$  would therefore depend on the used  $V_{\Delta}$  value, and consequently also  $v_p$ . To analyse this effect, the values of  $v_p$  have been estimated using two different voltage levels:  $V_{\Delta} = 1$  mV, which is equivalent to an

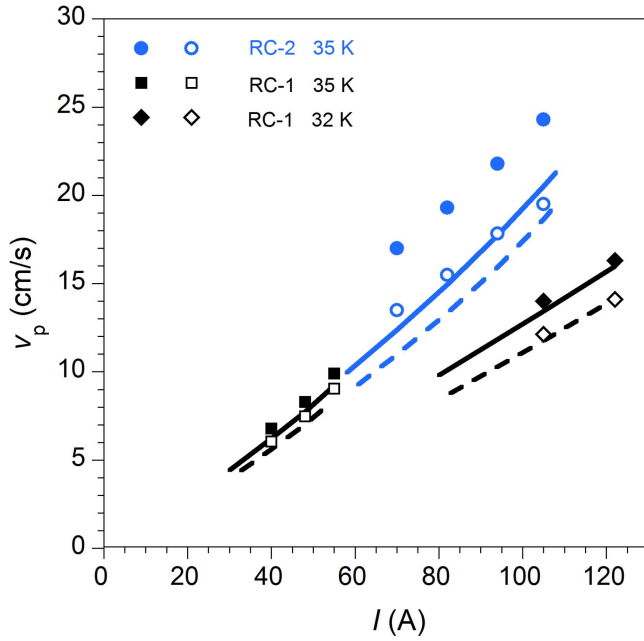


**Figure 4.** Quench propagation velocity in Rutherford cables RC-1 and RC-2 for different operating currents,  $I$ , and temperatures ( $T_0 = 32$  and  $35$  K). Symbols correspond to experimental values. Two set of data are given for each condition, corresponding to the values obtained using  $V_{\Delta t} = 1$  mV (solid symbols) or  $V_{\Delta t} = V_{\text{normal}}/2$  (open symbols), as explained in the text. Continuous lines are predictions by equation (1), Wilson's model; and discontinuous lines by Dresner's formula, equation (2).

electric field of  $\sim 0.8$  mV cm $^{-1}$  and is near the onset of the transition; and  $V_{\Delta t} = V_{\text{normal}}/2$ , where  $V_{\text{normal}}$  corresponds to the voltage in the normal state of the sensed strand segment, i.e.  $V_{\Delta t} \sim 15/2$  mV = 7.5 mV for a quench performed at operating current  $I = 82$  A.

Figure 4 displays  $v_p$  values obtained experimentally for cables RC-1 and RC-2 as a function of the operating current at different temperatures. The differences between  $v_p$  values estimated using both mentioned  $V_{\Delta t}$  levels, range between 10% and 25%.

During quench measurements of cable RC-1, it was observed that the zone of the cable at the right-hand side of the heater, around strand segment  $d-i$ , had lower critical current than the rest of the cable. Therefore, in this case, the time delay between voltages  $V_0(t)$  and  $V_2(t)$  were chosen to estimate  $v_p$ . For cable RC-2 it would be possible to use either  $V_2(t)$  or  $V_{2'}(t)$  to estimate global values of quench propagation velocities, and the differences between both values are also about 10%–25% depending on the current. Although these are global values, the quench propagation velocity may have significant local variations, as evidenced by the time delay between voltages  $V_1$  and  $V_{1'}$  seen in figure 2(b). It must be remarked that this behaviour is not unique to these MgB $_2$  cables, since differences in the local propagation velocity across the strands have also been reported for Nb–Ti Rutherford cables [21].

Analytical predictions for quench propagation in superconductors have been given by several authors. Wilson's model [25] assumes one-dimension geometry of the

conductor, which is represented during a quench by a normal conducting region adjacent to a superconducting region, with the transition between both at the temperature  $T_s$ . The temperature profile along the conductor is supposed to propagate at constant velocity,  $v_p$ , which in adiabatic conditions is given by:

$$v_p = \frac{I}{A} \frac{1}{c_v} \left( \frac{\rho_n k}{T_s - T_0} \right)^{1/2}, \quad (1)$$

where  $A$  is the area of the cross section (m $^2$ ),  $k$  the thermal conductivity (W m $^{-1}$  K $^{-1}$ ),  $c_v$  the heat capacity per unit volume (J m $^{-3}$  K $^{-1}$ ), and  $\rho_n$  the resistivity of the composite in the normal state ( $\Omega$  m).  $T_0$  is the initial temperature and  $T_s = (T_c + T_g)/2$ , is the mid-value between the critical temperature,  $T_c$ , and the temperature  $T_g$ , which is defined as the temperature at which the critical current equals the transport current,  $I = I_c(T_g)$ . Note that since  $T_g$  depends on the applied current, so does  $T_s$ . In Wilson's model,  $c_v$  and  $\rho_n$  are assumed constant (or averaged).

A similar equation is given by Dresner in [26], but in this case the strong temperature dependence of the specific heat is taken into consideration:

$$v_p = \frac{I}{A} \left( \frac{\rho_n k}{\Delta u_s c_v} \right)^{1/2}, \quad (2)$$

where  $\Delta u_s = u(T_s) - u(T_0)$  is the internal energy variation in the conductor, and  $k$ ,  $\rho_n$  and  $c_v$  are values at the transition temperature.

In the cables analysed in this study, the predictions given by Wilson and Dresner show rather good agreement with the experimental values. It is worth noting that despite of the simplifying assumptions of these models, they give valuable estimations of propagation velocities, at least as first approximations, not only for wires and tapes [23] but also for cables [27]. For example, recent studies by Manfreda *et al* [27] in quench propagation along Nb $_3$ Sn Rutherford cables concluded that predictions by Wilson's and Dresner's analytical models give close approximations, although they tend to overestimate the experimental values, mainly at lower temperatures (1.9 K), whereas at 4.2 K they give more accurate predictions, especially when using Dresner's equation.

There are some aspects to consider in the analysis of the experimental estimations of  $v_p$ . Ideally, it is preferable to estimate quench propagation velocities farther away from the heater, which is even more relevant in Rutherford cables, as during the first stages of quench development different velocities can be obtained from different individual strands [21, 27]. Nevertheless, in real experiments if longer distances from the heater are sensed to estimate  $v_p$ , the temperature of the hot-spot may also increase considerably depending on the sheath properties, and may cause the irreversible damage of the cable. In our experiments, maximum temperatures in the range between 50 and 65 K, depending on the operating current, have been measured by the TC during quench, without any apparent degradation of the cable. Nevertheless, the high electrical resistance of Cu10Ni alloy and the quasi-adiabatic conditions (sample in vacuum) result in an

insufficient thermal stability of these cables, which are prone to deteriorate if transition to the normal state occurs during high current operation. Therefore the introduction of higher conductive sheaths would be beneficial in terms of thermal stability and robustness during operation. For example, RC-2 was damaged irreversibly during critical current measurement at 33 K (this test was performed after having measured all quench measurements at 35 K).

### 3.3. Quench induced by overcurrents

As previously mentioned, the observed inhomogeneities in quench propagation could be caused by small inhomogeneities in the cabling structure and/or in the local  $I_c$ 's of strands. In order to analyse this effect, we have measured quench induced by overcurrents in sample RC-2. In this experiment there is not any external heat source, and the cable eventually quenches when a current higher than  $I_c$  is applied. In contrast to the quench activated by local heat sources at  $I < I_c$ , for overcurrents the transition to the normal state would initiate in unknown regions and it will propagate from there to the rest of the cable. Ideally, the quench would occur in all strands almost simultaneously if the current is distributed uniformly in all them and if there is homogeneity in temperature, cable structure and local critical currents. On the contrary, a lack of homogeneity or the existence of a temperature gradient in the sample would cause the quench to initiate at the weakest points of the cable.

The time evolution of the voltages measured in the different parts of the cable RC-2 is plotted in figure 5(a). In this experiment, the temperature of the cable was set to 35 K and, once stabilized, the current was increased up to 130 A  $> I_c(35\text{ K}) = 110\text{ A}$  at the maximum rate allowed by the power supply. At  $t = 0.4\text{ s}$  the set current was reached and kept constant. The apparition of a voltage of  $\sim 50\text{ }\mu\text{V}$ , which becomes unstable due to self-heating, eventually produces a quench. The whole cable does not quench at the same time, instead the quench was first detected in the central part of the cable by the coincident onset and values of  $V_0(t)$ ,  $V_{0,b}(t)$  and  $V_{\text{cable}}(t)$  curves. Shortly thereafter ( $\sim 5\text{ ms}$ ), the simultaneous onset of  $V_2(t)$  and  $V_1(t)$  marks the transition to normal state of these strand segments at the left-hand side of the cable. This is followed by the onset of  $V_2(t)$  and finally by  $V_1(t)$ .

Remarkably, some voltages measured between two different strands, could be negative, as seen in figure 5(a), behaviour also observed for cable RC-1. This is caused by the unequal quenching of the strands or strand segments, which causes local differences in  $E(J)$  between them (being  $E$  the local electric field and  $J$  the current density). In these cases, it is possible to measure transient negative voltages that will turn positive due to redistribution and transfer of current between strands and by the eventual transition to the normal state of the full sensed region.

Figure 5(b) shows the overall voltage in the cable,  $V_{\text{cable}}(t)$ , together with the sum of the voltages measured in several strand segments. Unlike the case of quench induced by a hot-spot, shown in figure 3(b), the overall voltage of the cable is not equal to the sum of these voltages in the full time

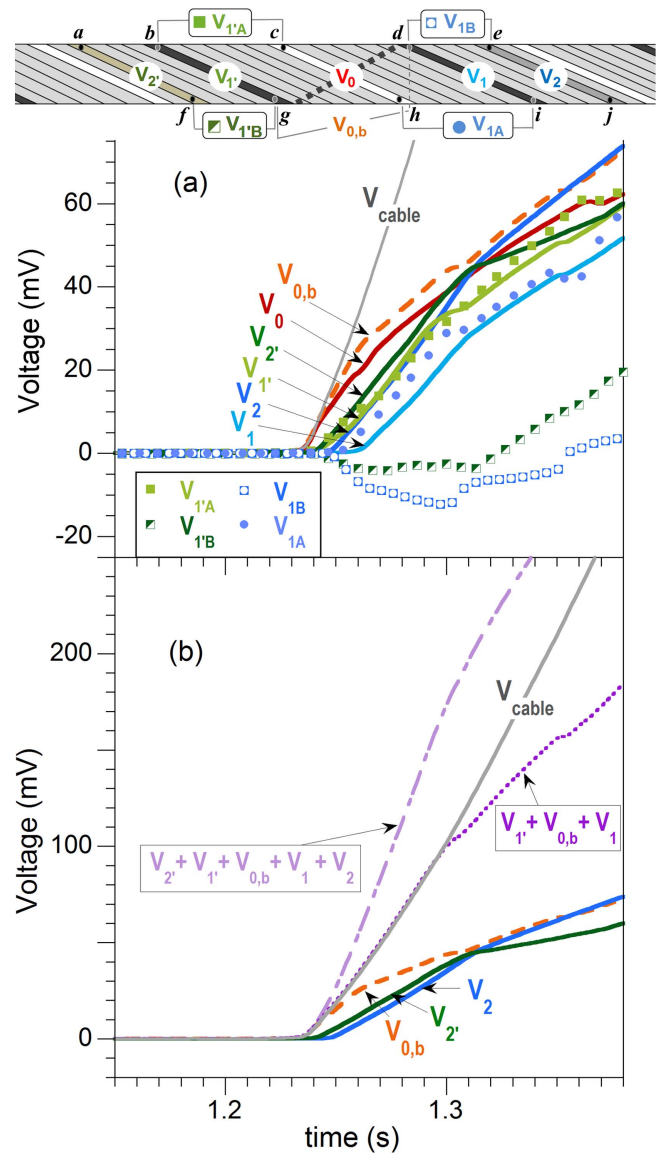


**Figure 5.** Time evolution of voltages measured in cable RC-2 at  $T_0 = 35\text{ K}$  and overcurrent  $I = 130\text{ A} > I_c = 110\text{ A}$ . (a) Voltages measured across strands (symbols defined in the inset), and along given strands (lines without symbols). (b) Comparison between the total voltage measured in the cable ( $V_{\text{cable}}$ ) with the sum of different voltages measured in several strand segments.

interval. This is in agreement with the measurement of negative values for inter-strands voltages, thus indicating that the quench does not propagate from the centre towards the ends, but instead it is produced by the nucleation of many normal zones distributed within the cable, i.e. different strand segments would quench almost simultaneously in different parts of the cable.

## 4. Conclusions

The analysis of the quench behaviour of  $\text{MgB}_2$  Rutherford cables has been presented. By careful measurement of the voltages measured along given strands and between strands, it



is possible to analyse the quench dynamics in these cables under local hot-spots and due to overcurrents.

In the case of quench induced by a local heat disturbance, we have observed two different time scales in the quench development. First, a slow dynamics for the formation of a MPZ, dominated by heat flow from the strand segments in contact with the heater to those at the bottom of the cable in contact with them. During this stage the heated strand segments are in the current-sharing regime, with the current shared between the superconducting core and the metal sheath. This time interval is considerably longer than for single conductors, which may be favoured by current redistribution among strands. Once a MPZ is developed, which is formed by segments of several strands, the quench propagates towards the ends of the cable in a shorter time scale.

The average quench propagation velocities estimated experimentally show a close correlation with the predictions given by one-dimensional-geometry models proposed by Wilson [25] and Dresner [26]. Nevertheless, there are important local variations of the quench propagation velocity across the strands near the hot-spot, also observed in LTS Rutherford cables. The presence of some inhomogeneities in the cable structure or local differences in  $E(J)$  among strands could cause these variations, which have also been observed in the case of quench produced by overcurrents.

For quench induced by overcurrents, we observed almost simultaneous nucleation of many normal strand segments surrounded by superconducting ones in different parts of the cable. These normal regions grow and collapse, resulting eventually in the transition of the entire cable.

The high electrical resistance of Cu10Ni alloy and the quasi-adiabatic conditions result in an insufficient thermal stability of these cables, which are prone to deteriorate if transition to the normal state occurs during high current operation. The introduction of a higher conductive sheath in the strands would be beneficial to make these cables more robust during operation.

## Acknowledgments

This work was supported by project ENE-2014-52105-R (from Spanish Ministerio de Economía, Industria y Competitividad and European FEDER Program) and by the Slovak Scientific Agency under the APVV-14-0522.

## ORCID iDs

P Kováč  <https://orcid.org/0000-0003-1872-0359>  
E Martínez  <https://orcid.org/0000-0003-4839-5286>

## References

- [1] Bottura L and Godeke A 2012 Superconducting materials and conductors: fabrication and limiting parameters *Rev. Accel. Sci. Technol.* **5** 25–50

- [2] Barzi E, Andreev N, Boffo C, Borissov E, Elementi L, Del Frate L, Yamada R and Zlobin A V 2004 Development and study of Rutherford-type cables for high-field accelerator magnets at Fermilab *Supercond. Sci. Technol.* **17** S213–6
- [3] Fleiter J, Ballarino A, Bonasia A, Bordini B and Richter D 2017 Optimization of Nb<sub>3</sub>Sn Rutherford cables geometry for the high-luminosity LHC *IEEE Trans. Appl. Supercond.* **27** 4004305
- [4] Collings E W, Sumption M D, Scanlan R M, Dietderich D R, Motowidlo L R, Sokolowski R S, Aoki Y and Hasegawa T 1999 Bi:2212/Ag-based Rutherford cables: production, processing and properties *Supercond. Sci. Technol.* **12** 87–96
- [5] Ha D-W *et al* 2008 Study on Bi-2212 Rutherford cabling process for SMES *IEEE Trans. Appl. Supercond.* **18** 1192–5
- [6] Hasegawa T *et al* 2001 Improvement of superconducting properties of Bi-2212 round wire and primary test results of large capacity Rutherford cable *IEEE Trans. Appl. Supercond.* **11** 3034–7
- [7] Kopera L, Kováč P, Hušek I and Melišek T 2013 Rutherford cable made of single-core MgB<sub>2</sub> wires *Supercond. Sci. Technol.* **26** 125007
- [8] Kopera L, Kováč P, Kulich M, Melišek T, Rindfleisch M, Yue J and Hušek I 2017 Critical currents of Rutherford MgB<sub>2</sub> cables compacted by two-axial rolling *Supercond. Sci. Technol.* **30** 015002
- [9] Kario A, Vojenciak M, Grilli F, Kling A, Ringsdorf B, Walschburger U, Schlachter S I and Goldacker W 2013 Investigation of a Rutherford cable using coated conductor Roebel cables as strands *Supercond. Sci. Technol.* **26** 085019
- [10] Kim H J, Seong K C, Cho J W, Bae J H, Sim K D, Kim S, Lee E Y, Ryu K and Kim S H 2006 3 MJ/750 kVA SMES system for improving power quality *IEEE Trans. Appl. Supercond.* **16** 574–7
- [11] Ohsemochi K *et al* 2006 Test results of an experimental coil with Bi2212 Rutherford cable for high energy-density HTS-SMES *J. Phys.: Conf. Ser.* **43** 825
- [12] Awaji S, Watanabe K, Oguro H, Miyazaki H, Hanai S, Tosaka T and Ioka S 2017 First performance test of a 25 T cryogen-free superconducting magnet *Supercond. Sci. Technol.* **30** 065001
- [13] Campbell A M 1982 A general treatment of losses in multifilamentary superconductors *Cryogenics* **22** 3–16
- [14] Martínez E, Yang Y, Beduz C and Huang Y 2000 Experimental study of loss mechanisms of AgAu/PbBi-2223 tapes with twisted filaments under perpendicular AC magnetic fields at power frequencies *Physica C* **331** 216–26
- [15] Wilson M N 2008 NbTi superconductors with low ac loss: a review *Cryogenics* **48** 381–95
- [16] Terzieva S, Vojenciak M, Pardo E, Grilli F, Drechsler A, Kling A, Kudymow A, Gömöry F and Goldacker W 2009 Transport and magnetization ac losses of ROEBEL assembled coated conductor cables: measurements and calculations *Supercond. Sci. Technol.* **23** 014023
- [17] Ghosh A K, Sampson W B and Wilson M N 1996 Minimum quench energies of Rutherford cables and single wire *IEEE Trans. Appl. Supercond.* **7** 954–7
- [18] Willering G P, Werweij A P, Kaugets J and ten Kate H H J 2008 Stability of Nb–Ti Rutherford cables exhibiting different contact resistances *IEEE Trans. Appl. Supercond.* **18** 1263–6
- [19] Collings E W, Sumption M D, Susner M A, Dietderich D R, Krooshoop E and Nijhuis A 2012 Interstrand contact resistance and magnetization of Nb<sub>3</sub>Sn Rutherford cables with cores of different materials and widths *IEEE Trans. Appl. Supercond.* **22** 6000904



- [20] Fleiter J, Bordini B, Ballarino A, Oberli L, Izqueirido S and Bottura L 2015 Quench propagation in Nb<sub>3</sub>Sn Rutherford cables for the Hi-Lumi quadrupole magnets *IEEE Trans. Appl. Supercond.* **25** 4802504
- [21] Willering G P 2009 Stability of superconducting rutherford cables for accelerator magnets *PhD Thesis* University of Twente, The Netherlands
- [22] Willering G P, Verweij A P and Ten Kate H H J 2008 Current redistribution around the superconducting-to-normal transition in superconducting Nb–Ti Rutherford cables *J. Phys.: Conf. Ser.* **97** 012119
- [23] Martínez E, Lera F, Martínez-López M, Yang Y, Schlachter S I, Lezza P and Kováč P 2006 Quench development and propagation in metal/MgB<sub>2</sub> conductors *Supercond. Sci. Technol.* **19** 143–50
- [24] Ye L, Cruciani D, Xu M, Mine S, Amm K and Schwartz J 2015 Magnetic field dependent stability and quench behavior and degradation limits in conduction-cooled MgB<sub>2</sub> wires and coils *Supercond. Sci. Technol.* **28** 035015
- [25] Wilson M N 1983 *Superconducting Magnets* (Oxford: Clarendon)
- [26] Dresner L 1995 *Stability of Superconductors (Selected Topics in Superconductivity)* (New York: Plenum)
- [27] Manfreda G, Bellina F, Bajas H and Perez J C 2016 Analysis of the quench propagation along Nb<sub>3</sub>Sn Rutherford cables with the THELMA code: II. Model predictions and comparison with experimental results *Cryogenics* **80** 364–73